

# Optical Force/Tactile Sensors for Robotic Applications

*Marco Costanzo and Salvatore Pirozzi*

**N**owadays, robotic systems use tactile sensing as a key enabling technology to implement complex tasks. For example, manipulation and grasping problems strongly depend on the physical and geometrical characteristics of the objects; in fact, objects may be deformable or change their shape when in contact with the robot or the environment. For this reason, often, robots end effectors are equipped with sensorized fingers which can estimate the objects' features, forces, and contact locations. This is useful in a safe and efficient physical Human-Robot Interaction (pHRI) to perform cooperation and co-manipulation tasks while limiting damage from accidental impacts.

Currently, the manipulation abilities of modern robots are far from human dexterous manipulation skills. A grasping device should be able to firmly grasp any kind of object without damaging it. This can be done by controlling the grasping force which again requires accurate estimates of contact forces and moments. Tactile sensors are of paramount importance in dexterous robotic manipulation, and they should be able to detect gross and incipient slippage and measure friction on contact with an object. Research in [1] surveys the field of tactile sensing from this point of view.

The use of tactile sensors in robotics is not limited to manipulation tasks. In [2], the authors use tactile sensing to recognize the nature of unknown surfaces by exploiting bimorph piezoceramic actuators and sensors to stimulate a surface and measure the response. Research in [3] considers the capacitive variations in commercial piezoresistive transducers to sense applied pressure for hand exoskeletons. Instead, [4] proposes tactile feedback for human-computer interaction with an emphasis on foot-based interfaces. Tactile data are also used to solve classification problems such as object recognition; as an example, [5] investigates tactile data as time sequences to solve object recognition problems.

This paper reviews the evolution of the tactile sensing technology developed at the Robotics Lab of the University of

Campania Luigi Vanvitelli. The paper first describes the hardware technology and its evolution in the last decade. Then, the work shows how, by means of the tactile measurements, it is possible to reconstruct the contact wrench through an Artificial Neural Network (ANN) and/or to estimate the shape of an object. Finally, some advanced robotic applications are shown. By using force/torque estimation it is possible to both automatically choose the grasp force that avoids the slippage and control the in-hand sliding motion of the object between the fingers to change the relative pose between the fingers and the grasped object. Instead, by using the shape recognition ability, it is possible to estimate the current shape of a grasped cable to correctly align the cable tip to the hole of a switchgear in an autonomous assembly task.

## The Sensing Technology Evolution

The idea of designing and developing, in our laboratories, a tactile sensor based on optoelectronic technology dates to about a decade ago, within the European research project DEXMART. During recent years, the evolution of optoelectronic devices and our experience in the field allowed us to optimize our prototypes, achieving in the latest versions a high measurement performance and a high mechatronic integration level. The working principle (reported the first time in [6]) is based on the design of a deformable layer to be suitably assembled with a discrete number of optoelectronic sensing devices, with the objective to transduce the external contacts into deformations measured by optical sensible points (typically called "taxels" in literature). The sensing points, positioned below the deformable layer, provide a "tactile map" corresponding to spatially distributed information about the contact. Based on application task, the tactile map can be used to reconstruct contact properties, e.g., contact force, contact torque, object shape.

The first version [6] comprised only two layers: an optoelectronic layer (i.e., a Printed Circuit Board—PCB) and a deformable one. Each sensing point was realized by using a

---

This work was supported by the European Commission within H2020 REFILLS Project (no. 731590) and H2020 REMODEL Project (no. 870133).

couple of optoelectronic components manufactured by OSRAM: an infrared LED (code SFH480) with a typical peak wavelength of 880 nm and a silicon NPN phototransistor (code SFH3010) with a maximum peak sensitivity at 860 nm. The collector current was directly translated into a voltage signal by using a simple resistor. A matrix of 4x4 taxels with a spatial resolution of 2 mm was implemented. The 16 voltage signals, representing the tactile map, were digitalized with an Analog-to-Digital (A/D) converter chip (code AD7490, 12-bit, 16 channels) with an SPI interface. The voltage supply of all sensor components was 3.3 V with a maximum power consumption of 200 mW. The deformable layer was made of black silicone to avoid ambient light disturbances and cross talk among nearby taxels. Only the surface in front of the optoelectronic devices was white in order to increase the sensitivity. Finite Element analysis has been used to optimize the design of deformable layer geometry. The realized layer had a square base with dimensions equal to 11.4 × 11.4 mm, and the top was a section of a sphere with a radius of 11.4 mm. The silicone was a hardness of 9 Shore A, resulting into a force measurement range equal to [0,4] N. The main application was the integration into an anthropomorphic robotic hand.

A first objective for the evolution of the proposed tactile sensing technology was the realization of a spatial extended version, useful for an application in which an artificial skin is required. During the SAPHARI European project, an extended and conformable prototype was developed and tested for physical human–robot interaction [7]. To this aim a modular structure was selected, where the single module comprised a 2 × 2 matrix of taxels and a silicone cup, and it was realized with the same approach, components and materials used in [6]. However, in order to realize a wide and conformable sensing patch, 36 of these modules were realized on a single flexible PCB with as many silicone cups, and they have been suitably assembled (as a 6 × 6 matrix of modules) to obtain an artificial skin patch with a total of 144 taxels and an active surface of about 47 × 47 mm<sup>2</sup>. The acquisition of a high number of taxels, without the need for as many A/D channels, requested the use of an external MicroController Unit (MCU) with a specific “scanning control” strategy. The scanning strategy provided the following phases: to connect the sensing modules in groups which share 4 A/D channels; to switch on and off the sensing modules by using the digital I/O of the microcontroller, with a cyclic pattern; and the cyclic pattern ensured that at a fixed time instant, only one taxel for each group was turned on, while the others, sharing the same A/D, were turned off. The strategy worked well since the switched off photodetectors behave as an open circuit, without influencing the A/D conversion, and MCU digital I/O were able to drive the sensing modules, since the LEDs worked with a forward current of about 1 mA and a voltage supply of 3.3 V.

More recently a new version of tactile sensor has been optimized to be integrated in a commercial parallel gripper for robotic systems [8] within the REFILLS European project. This version comprises three layers: an optoelectronic PCB, a rigid mechanical grid, and a deformable layer. Several improvements

with respect to previous versions have been introduced. First, the LED/phototransistor couple has been substituted by a unique optoelectronic component: the NJL5908AR photo-reflector, manufactured by New Japan Radio. This device, constituted by an infrared LED (with a peak wavelength at 920 nm) and a phototransistor (with a peak wavelength at 880 nm), guarantees a higher sensitivity to light reflection, and it allows a high reduction of taxel mechanical uncertainties related to the relative orientation among the separate optoelectronic devices used in previous versions. Consequently, the taxel behaviors became more uniform and with a deeper range of measurement, by increasing the overall sensor performance. Additionally, the sensitive area has been increased, to manipulate a larger number of objects, by increasing the number of taxels and the spatial distance among them. In detail, the PCB integrates a 5 × 5 matrix of taxels, with a spatial distance of 3.55 mm, resulting in a sensitive area equal to 21.3 × 21.3 mm<sup>2</sup>. The digitalization of taxel signals has been implemented by using a couple of the same 12-bit A/D converters with SPI interface that were previously used. Moreover, a microcontroller section (based on a PIC16F1824, manufactured by Microchip Technology) has been added to the PCB design, with the objective to realize a fully integrated sensorized finger, with a programmable device, which allows the sensor interrogation by using a standard serial interface, typically available in most commercial grippers. The input stage of the PCB is completed with a standard low-noise voltage regulator (input voltage up to 12 V from the gripper, output voltage 3.3 V for the PCB). The deformable layer is very similar to the previous version in terms of materials and design but simply scaled to new taxel matrix. As mentioned, when objects come in contact with the deformable layer, they produce vertical deformations of the cell white surfaces. These distance variations correspond to variations of the reflected light and consequently of the measured voltage signals. Since the NJL5908AR photo-reflector has a non-monotonic distance-voltage characteristic, the rigid grid, introduced in this version, has become fundamental so that the reflecting surfaces never reach distances that fall into the non-monotonic area of the optomechanical characteristic of the components. The grid presents holes suitably designed to house rigid pins, which are bonded to grid via a cyanoacrylate glue, and then the assembled grid is bonded to the deformable layer. The rigid pins are used for the mechanical assembly with the optoelectronic layer. The PCB presents suitable holes used for the alignment and the connection of the mechanical structure constituted by the deformable layer and the rigid grid (by soldering the pins on the PCB). The obtained sensor can be integrated into a case suitably designed to be used as a sensorized finger for a parallel gripper. The assembled sensor can be interrogated via a standard serial interface with a maximum sampling rate equal to 500 Hz.

A similar version has been developed within the WIRES experiment implemented during the ECHORD++ European project. During this experiment, for the first time, a tactile sensor with a flat surface and a very small thickness has been realized for the shape recognition of deformable objects (i.e., cables) and their manipulation in narrow space [9]. The sensing

matrix comprises 16 photoreflectors NJL5908AR with a spatial resolution equal to 3 mm and a distance from PCB edges equal to 2 mm, by obtaining a total size for the PCB equal to 13 mm. A single A/D converter (AD7490) with an on-board microcontroller (PIC16F1824) have been used to complete the board. A standard serial interface with a sampling rate of 500 Hz is used to interrogate the sensor. As described, the deformable layer has been designed with a flat top side, while the bottom side presents 16 square cells with a reflective surface of 2 mm side and intermediate black walls with 1 mm side. The edges of the deformable layer are 2 mm thick, so that the total size of the sensitive flat area is  $15 \times 15 \text{ mm}^2$ . The rigid grid has been realized in ABS via 3D printing technology, by reducing its thickness to the minimum functional value (0.8 mm). A suitable aluminum case realized via 3D printing technology has been designed to house the sensor by maintaining a minimum thickness. All layers have been bonded among them and into the case, by obtaining a final prototype with a total thickness for the tip less than 6 mm. The used silicone has a shore hardness of 26 A, corresponding to a maximum applicable normal force up to 30 N, with a resolution of 0.3 N and about 10% of hysteresis.

During last two years, within the European projects RE-FILLS and REMODEL, a completely new design for the PCB board has been developed in order to increase the measurement performance of the sensor, by modifying the LED driving and the phototransistor signals acquisition [10]. The selected optical components are the same (NJL5908AR) and also the spatial distribution (a  $5 \times 5$  matrix with a distance among taxels equal to 3.55 mm), by obtaining a sensitive area equal to about  $22 \times 22 \text{ mm}^2$ . However, while in the previous version LEDs were parallel driven with a voltage supply, in this design the LEDs are in series and current driven through an adjustable current source (LM334) in order to increase emitted light stability, by reducing its drift due to temperature and power supply noise. Additionally, analog buffers have been introduced to decouple the photoreflector voltage signals from the A/D converter stage. They have been realized by using the low power operational amplifiers ADA4691 and used to directly connect signals to a PIC microcontroller (PIC16F19175) with integrated 12-bit A/D channels. This solution (without a separate A/D device with SPI interface) allowed a simplification of the interrogation firmware and an enhancement of the signal-to-noise ratio. All components are integrated into a single PCB, by obtaining a fully integrated sensor with a programmable device used for data acquisition. In addition to a standard serial interface with a sampling frequency equal to 500 Hz, an alternative interface (e.g., SPI, I2C, Wireless) can be implemented. The rigid grid has been re-designed in order to exploit PCB edges for the alignment with the optoelectronic components and for the bonding. The deformable pad can be realized with different shapes on the basis of the application scenario. A flat surface can be well exploited if the object shape recognition is requested for the task implementation. Instead, if the robotic task needs information about contact forces and moments, it is possible to reconstruct them from the tactile image by using a domed deformable layer with a suitably trained neural network, as better described

below. Domed cups with different curvature radii allow different performance in terms of reconstructed forces and stability of contact area to be obtained. Fig. 1 reports the timeline of the tactile sensing technology evolution through the years and the European projects, providing pictures and the main features of the prototypes described in this section.

## Sensor Measurements and Characterization

All described prototypes, in rest condition, measure for each  $i$ -th taxel a positive offset voltage  $v_i(0)$ . If contact with external objects occurs, the taxel shows a voltage variation  $\Delta v_i(t) = v_i(t) - v_i(0)$ , related to the deformable layer deformations. The voltage measurements  $\Delta v_i$  correspond to the tactile map available as sensor output. From a graphical point of view, in order to report  $\Delta v_i$  amplitudes, two possible representations can be used: a first representation which reports the voltage variation as a red circle with radius proportional to the acquired  $\Delta v_i$ ; and a second representation which uses a matrix of cells whose colors change with  $\Delta v_i$ , according to a defined colorbar. This tactile map can be directly used for object shape recognition or elaborated to estimated derived quantities such as contact force and torque components, to exploit in feedback control systems. Fig. 2 reports some examples of typical voltage signals and tactile maps used for the reconstruction of a grasped wire shape and a pen. The figure shows both possible map representations for different prototypes. The sensor measurement performance mainly depends on the mechanical properties of the material and the shape of the deformable layer and by the operating points and optical characteristics of the optoelectronic devices. With the aim to characterize the properties of proposed tactile sensor, since tactile commercial solutions are not available as reference sensors, a 6-axis force/torque sensor (manufactured by ATI) has been used as reference. This paper reports the characteristics of the most recent version presented above, assembled with the reference sensor as reported in Fig. 2. For example, the hysteresis can be evaluated by comparing the voltage variation  $\Delta v_i$  for a taxel with respect to normal force  $f_z$  measured by the reference sensor. From the data, reported in Fig. 2, a hysteresis mean error of about 10% has been computed, also by considering different velocity in force application. By using the characterization setup, additional properties can be easily derived, such as the repeatability in terms of  $\Delta v_i$  obtained by applying the same force profile, which presents a maximum error less than 7%. The time response has been evaluated by applying a force with a step change to the sensor: the obtained value is less than 1ms. Moreover, by computing the Power Spectral Density of a typical voltage signal, it is possible to evaluate that the noise level is below the signal level of about four orders of magnitude.

The contact interaction between the sensor pad and an item is not described only by a tactile map, but also by friction forces and torques. Such quantities are of paramount importance during a grasp; indeed, the friction measurement can be used to conveniently choose the grasp force, both to firmly grasp an object and to allow controlled sliding.



**Fig. 1.** Evolution of proposed tactile sensing technology. This figure uses some material, with permission, from [6] (©2012 Elsevier), [7] (©2016 IEEE), [8] (MDPI Open Access), [9] (©2018 IEEE), [10] (©2020 IEEE).



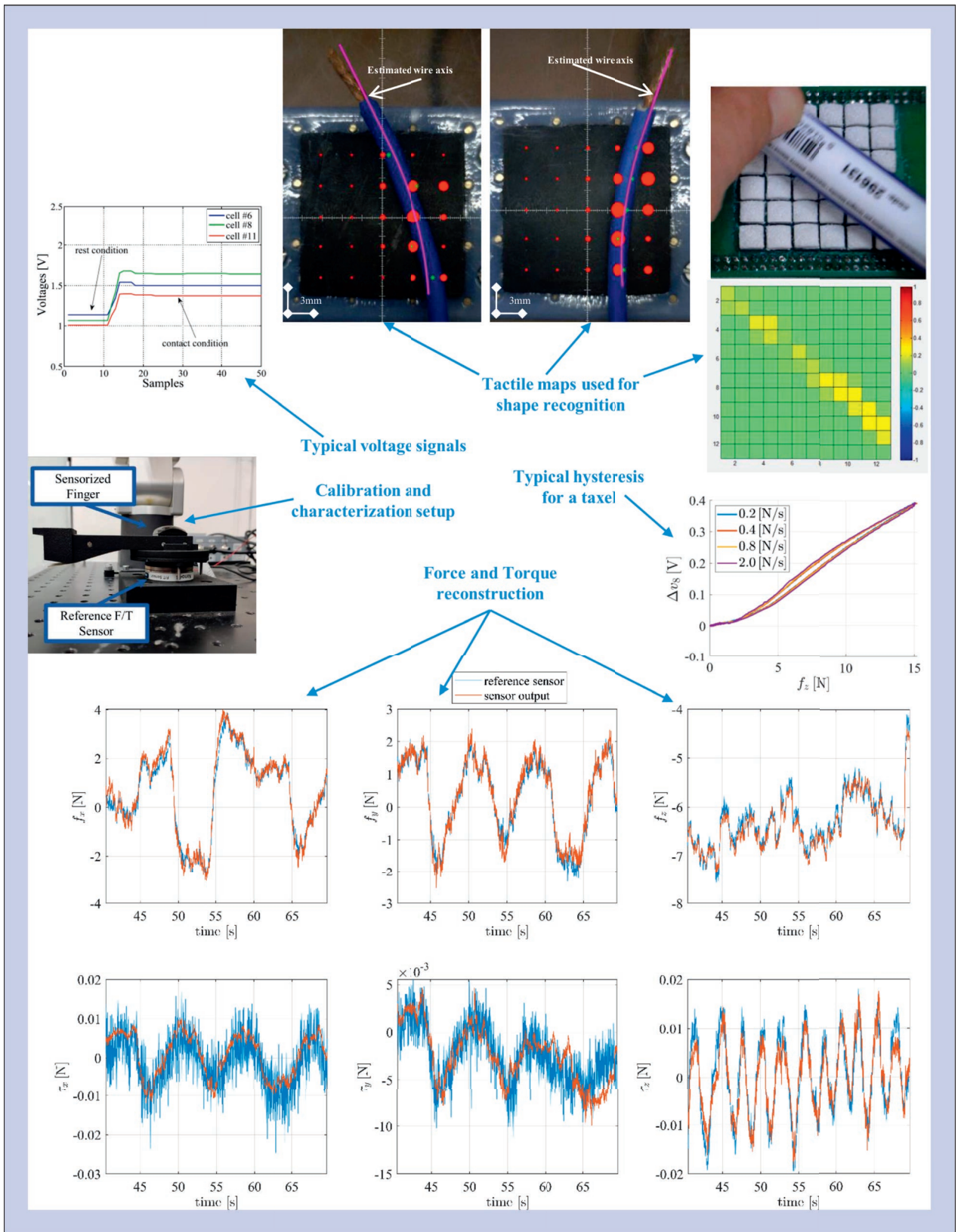


**Fig. 2.** Tactile sensor characterization. This figure uses some material, with permission, from [9] (©2018 IEEE) and [10] (©2020 IEEE).

As said, the force applied to the sensor causes a deformation of the pad and, in turn, a change in the measured tactile map. Moreover, the use of a non-axisymmetric shape for the deformable layer implies, in the presence of torsional moments, the generation of the torsional warping effect, which is measurable by the tactile map and guarantees the estimation of the applied torques. Here, a summary of the procedure, to invert this relationship and estimate the applied force by knowing the tactile map, is reported. The mapping is provided by training an Artificial Neural Network (ANN). The critical point of this procedure is the training data collection.

The ANN should be able to estimate the contact force and torque in all of the possible force/torque combinations applied in all possible points of the sensor pad. The dimensionality of the problem is large; thus, we need a specific procedure to acquire the data. The detailed procedure is described in [8]. To collect the data, the sensor is mounted on a reference force/torque sensor (Fig. 2). Various forces and torque combinations are applied on the pad by using a rigid object, and the measured force and the corresponding tactile map is stored. In [8], a MATLAB GUI helps the user visualize the data and the calibration status in order to apply all possible force combinations. The data are first post-processed to reduce the problem dimensionality and the sample number, and then they are used to train a Feed-Forward ANN. The network is made of six hidden layers, and each hidden layer is made of 90 neurons and a sigmoidal activation function. Fig. 2 shows an example of force-torque reconstruction, where the force is reconstructed with a mean error of 0.2 N and the torque with a mean error of 0.002 Nm.

## Robotic Applications

This section reports three possible robotic applications for the proposed sensing solution. As already stated, the ability to measure the force applied to the sensor pad can be used in grasping applications to avoid or control the slippage of a grasped object. These abilities can be performed by simple parallel jaw grippers equipped with the sensors. Here, two manipulation abilities based on the reconstructed forces and torques are described: the slipping avoidance and the pivoting. The first consists of firmly grasping an object by applying the “slowest” grasp force that avoids slippage. The second one consists of letting the object rotate between the fingers to change the relative orientation between the gripper and the object. Both abilities are provided via a model-based approach described in [11]. The contact is modeled via the rototranslational extension of the Coulomb friction law, i.e., the Limit Surface [12], while the slipping dynamic is described with a LuGre friction model [13].

The details about slipping avoidance algorithm are described in [14] and [15]. The control algorithm is represented in Fig. 3a, comprised of two control actions: a static control action that provides the minimum grasp force in static condition by exploiting the Limit Surface theory; and a dynamic action that computes the grasp force needed when the force varies rapidly (e.g., when a robot arm lifts an object from a table) and it is based on a nonlinear slippage observer. Fig. 3b shows an example, in which the plot reports the measured tangential

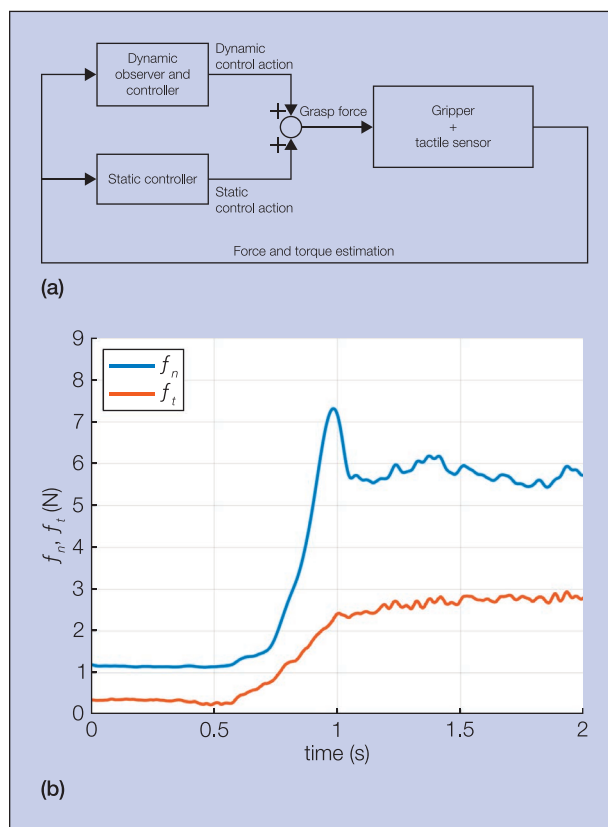


**Fig. 3.** Slipping Avoidance. (a) Control Scheme and (b) an experimental example, illustrating tangential force  $f_t$  (red line) and actuated grasp force  $f_n$  (blue).

force  $f_t$  and the grasp force  $f_n$  during a lift maneuver. As soon as the lift begins, the tangential force increases because the sensor feels the object weight, and at the same time, the slipping control algorithm automatically computes the normal force needed to lift the object. The lift was successful without any noticeable slip. Note that the algorithm can also deal with the torsional moment, as detailed in the cited papers.

The second example, the pivoting algorithm, is detailed in [11] and [15]. This maneuver can be executed in two different modalities called gripper and object pivoting, respectively. The first one consists of having the object fixed in the space while the gripper rotates about the grasp axis so as to change the relative orientation between the gripper and the object. An example is depicted in Fig. 4a, in which the object has to be placed in the narrow space between the two shelves on the right, and the motion is infeasible in the initial configuration because of collisions with the top shelf. By letting the gripper rotate with respect to the object, it is possible to reach the new grasp configuration that makes the grasp feasible.

The second pivoting modality is the dual one and consists of having the gripper fixed in the space while the object rotates in a pendulum-like motion. An example is depicted in Fig. 4b, where the bottle has been grasped, for some reason, in the depicted horizontal orientation and has to be placed vertically. The motion is feasible only if the robot has a large workspace and it is able to place the object from the top. By letting the

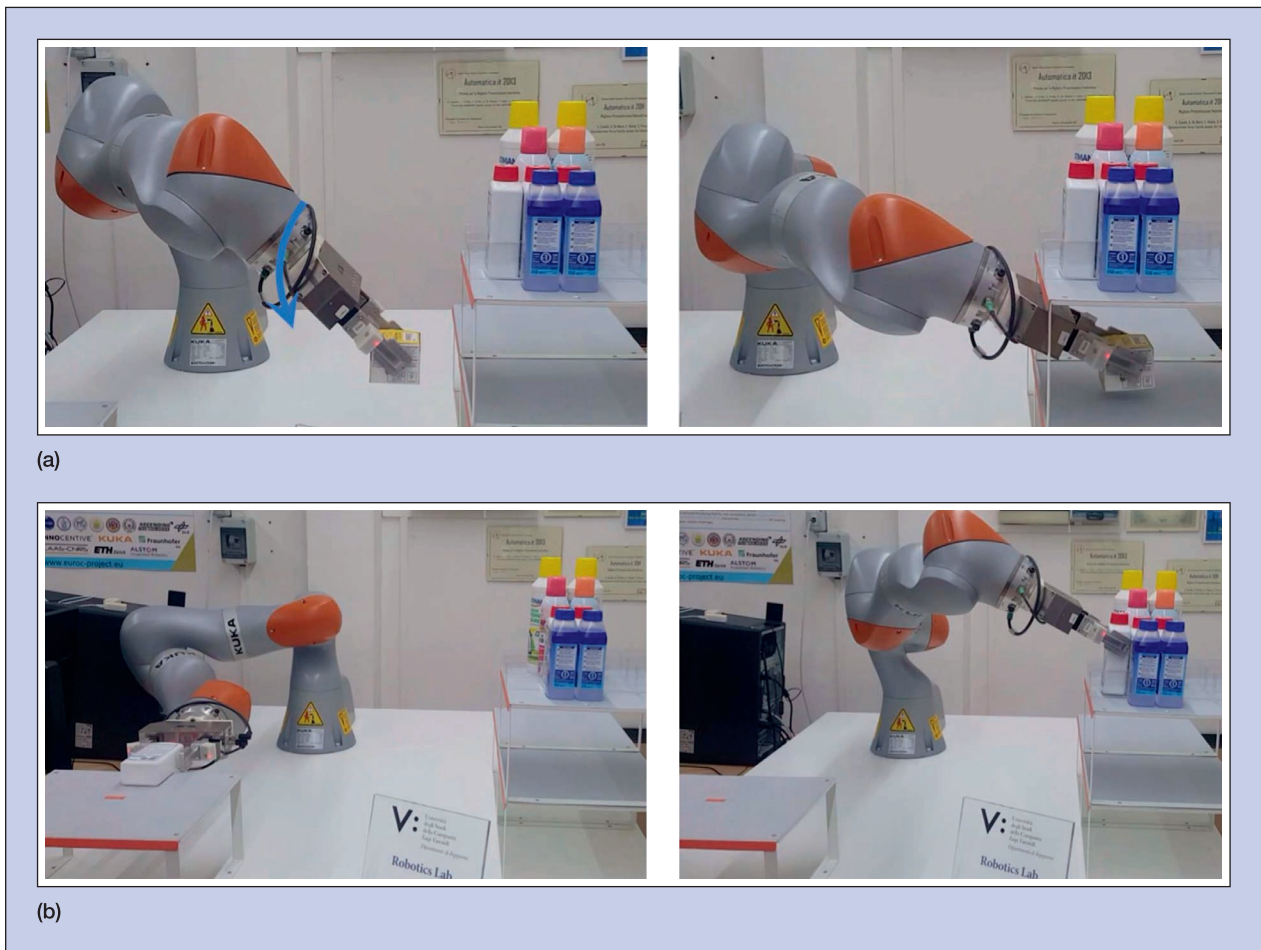


Fig. 4. (a) Examples of Gripper Pivoting. (b) Examples of Object Pivoting.

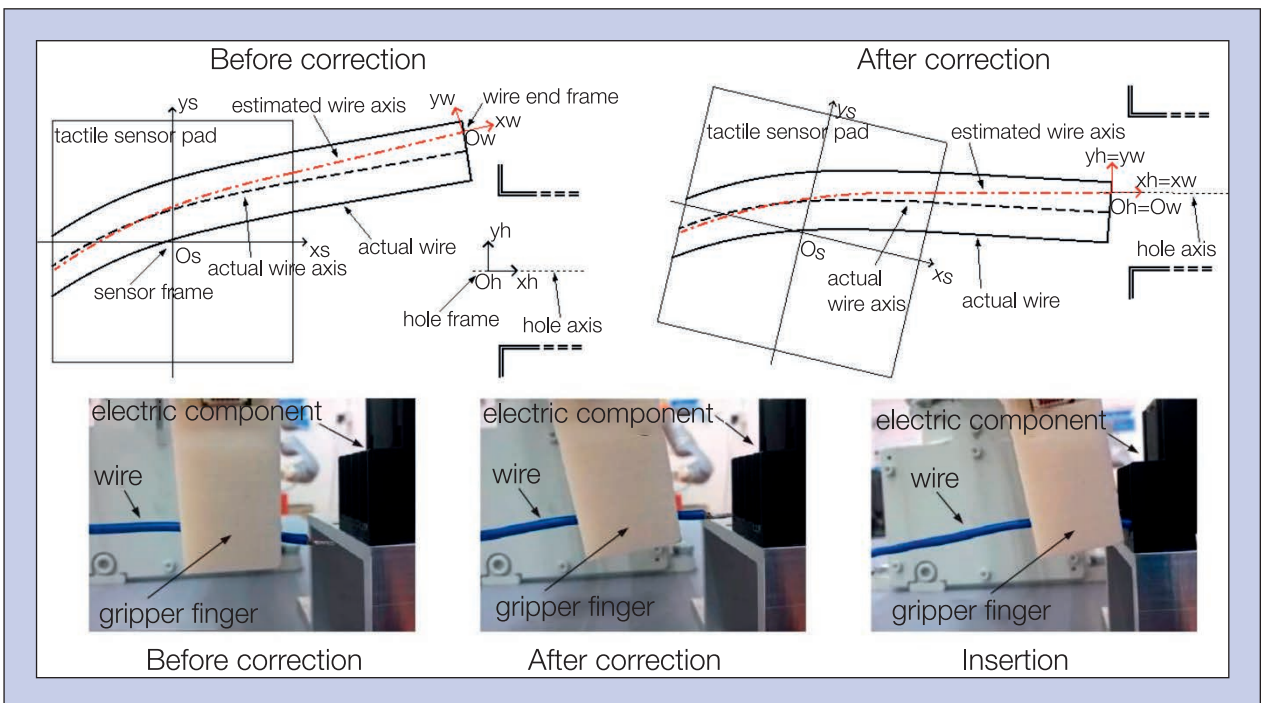


Fig. 5. Sketch and pictures of a wire insertion task. The figure uses some material, with permission, from [9] (©2018 IEEE).



object rotate in-hand, it is possible to reach a vertical orientation without moving the robot, making the task much easier.

Flat solutions are being used in the REMODEL European project for the manipulation of Deformable Linear Objects (DLOs), in particular for cables. One of the project use cases is the automated assembly of switchgears. A fundamental task in the assembling phase is the insertion, with the following mechanical connection, of the wire tip into the holes of the electromechanical components, constituting the switchgear. For the correct implementation of this task, under the assumptions to know the positions of the sensor reference frame and of the hole frame, it is possible to estimate a wire end frame, on the basis of the tactile map. By aligning the wire end frame with the hole frame, it is possible to correctly complete the task. Additional assumptions concern the initial positioning of the wire to grasp, which must ensure that the length of the protruding part for the grasped wire remains almost constant. The whole task can be executed as four subtasks: wire grasping from its initial position, approaching to the hole frame, correction of wire position and orientation on the basis of estimated wire end frame, and final insertion. The tactile data are used for the implementation of the correction subtask, without which the insertion can be completed. In detail, the tactile map is used to estimate the parameters of a quadratic model that approximates the shape of the grasped wire. By knowing, from the assumptions, the length of the protruding part, the parameters of this part can also be estimated by fixing an estimated wire end frame on the tip of the wire. In Fig. 2, an example of wire shape estimation is shown, while Fig. 5 reports a sketch and pictures from an experiment about how the estimated frame is used. In particular, the estimated wire end frame is used to correct the robotic trajectory in order to align this frame with the hole frame, so that the final insertion can be completed. Finally, note that the same tactile sensor data can be used to check if during the insertion, unexpected contact occurs and if after the screwing, the wire result is firmly connected [9].

## Conclusions

This paper presented the evolution of tactile sensing technology and the associated control methodology developed in our laboratory. Tactile sensing is of paramount importance in unstructured scenarios where the robot has to grasp objects of unknown weight or deformable objects that change their shape as soon as they are grasped. We showed how it is possible to combine our tactile sensors at fingertips and suitable estimation and control algorithms to manipulate both an object in a pick-and-place operation and a deformable cable in an automated assembly task.

## References

- [1] W. Chen, H. Khamis, I. Birznieks, N. F. Lepora and S. J. Redmond, "Tactile sensors for friction estimation and incipient slip detection—toward dexterous robotic manipulation: a review," *IEEE Sensors J.*, vol. 18, no. 22, pp. 9049-9064, Nov. 2018.
- [2] S. Baglio, G. Muscato N. Savalli, "Tactile measuring systems for the recognition of unknown surfaces," *IEEE Trans. Instrum. Meas.*, vol. 51, no. 3, pp. 522-531, Jun. 2002.
- [3] A. Damilano, A. Lince, S. Appendino, H. M. A. Hayat, P. Ariano, D. Demarchi, M. Crepaldi, "Commercial tactile sensors for hand exoskeletons: practical considerations for ultra-low cost and very-low complexity read-out," *IEEE Instrum. Meas. Mag.*, vol. 19, no. 5, pp. 49-56, Oct. 2016.
- [4] R. Velázquez, E. Pissaloux, C. Del-Valle-Soto, A. Lay-Ekuakille B. Andò, "Usability evaluation of foot-based interfaces for blind travelers," *IEEE Instrum. Meas. Mag.*, vol. 23, no. 4, pp. 4-13, Jun. 2020.
- [5] H. Liu, D. Guo F. Sun, "Object recognition using tactile measurements: kernel sparse coding methods," *IEEE Trans. Instrum. Meas.*, vol. 65, no. 3, pp. 656-665, Mar. 2016.
- [6] G. De Maria, C. Natale, and S. Pirozzi, "Force/tactile sensor for robotic applications," *Sensors Actuators A: Phys.*, vol. 175, pp. 60-72, 2012.
- [7] A. Cirillo, F. Ficuciello, C. Natale, S. Pirozzi, and L. Villani, "A conformable force/tactile skin for physical human-robot interaction," *IEEE Robotics and Automation Letters*, vol. 1, pp. 41-48, 2016.
- [8] M. Costanzo, G. De Maria, C. Natale, and S. Pirozzi, "Design and calibration of a force/tactile sensor for dexterous manipulation," *Sensors MDPI*, vol. 19, no. 4, 2019.
- [9] S. Pirozzi and C. Natale, "Tactile-based manipulation of wires for switchgear assembly," *IEEE/ASME Trans. Mechatronics*, vol. 23, no. 6, pp. 2650-2661, 2018.
- [10] M. Costanzo, S. Stelter, C. Natale, S. Pirozzi, G. Bartels, A. Maldonado and M. Beetz, "Manipulation planning and control for shelf replenishment," *IEEE Robotics and Automation Letters*, vol. 5, no. 2, pp. 1595-1601, 2020.
- [11] A. Cavallo, M. Costanzo, G. De Maria, and C. Natale, "Modeling and slipping control of a planar slider," *Automatica*, vol. 115, May 2020.
- [12] S. Goyal, A. Ruina, and J. Papadopoulos, "Planar sliding with dry friction, part 1—limit surface and moment function," *Wear*, vol. 143.2, pp. 307-330, 1991.
- [13] K. Johanastrom and C. Canudas De Wit, "Revisiting the LuGre friction model," *IEEE Control Syst. Mag.*, vol. 28.6, pp. 101-114, 2008.
- [14] M. Costanzo, G. De Maria, and C. Natale, "Slipping control algorithms for object manipulation with sensorized parallel grippers," *IEEE Int. Conf. Robotics and Automation (ICRA)*, pp. 7455-7461, 2018.
- [15] M. Costanzo, G. De Maria, and C. Natale, "Two-fingered in-hand object handling based on force/tactile feedback," *IEEE Trans. Robotics*, vol. 36.1, pp. 157-173, 2020.

**Marco Costanzo** (marco.costanzo@unicampania.it) is currently a Research Fellow at the University of Campania Luigi Vanvitelli, Italy. He received the Ph.D. degree in 2021 in Industrial and Information Engineering with a thesis on in-hand manipulation and the master's degree in 2017 in Information Engineering. His research interests include advanced robotic manipulation by using force/tactile sensing, as well as multi-modal sensing for safe human-robot interaction.

**Salvatore Pirozzi** (salvatore.pirozzi@unicampania.it) is an Associate Professor with the University of Campania Luigi Vanvitelli, Italy. His research interests include design and modelling of innovative sensors, in particular of tactile solutions, as well as interpretation and fusion of data acquired from the developed sensors.